Low-Temperature and Solventless Ring-Opening Polymerization of Eutectic Mixtures of l-Lactide and Lactones for Biodegradable Polyesters

Castillo-Santillan, Martín; Maniar, Dina; Gutiérrez, María C.; Quiñonez-Angulo, Priscila; Torres-Lubian, José Román; Loos, Katja; Mota-Morales, Josué D.

Published in:
ACS Applied Polymer Materials

DOI:
10.1021/acsapm.3c00591

Publication date:
2023

ACS APPLIED POLYMER MATERIALS

pubs.acs.org/acsapm Article

Low-Temperature and Solventless Ring-Opening Polymerization of Eutectic Mixtures of L-Lactide and Lactones for Biodegradable Polyesters

Martín Castillo-Santillan, Dina Maniar, María C. Gutiérrez, Priscila Quiñonez-Angulo, José Román Torres-Lubian, Katja Loos,* and Josué D. Mota-Morales*

Cite This: ACS Appl. Polym. Mater. 2023, 5, 5110−5121 Read Online

ACCESS | Metrics & More | Article Recommendations | Supporting Information

ABSTRACT: Biodegradability is one of the key features for reducing the negative environmental impact of plastic waste disposal; therefore, designing biocompatible polymeric biomaterials with programmable life cycles is urgently needed. Herein, deep eutectic solvent monomers (DESm) composed of L-lactide and various lactones of different molecular weights were formulated to obtain polyesters at low temperatures with the aid of organocatalysts and under solventless conditions. The introduced DESm expand the range of eutectic mixtures capable of undergoing ring-opening polymerization (ROP) to include mixtures of L-lactide with δ-valerolactone and δ-hexalactone. Extending the toolbox for DESm preparation will allow for the design of polyesters with tailored molecular weight and crystallinity, which are conducive to programmable degradability. ROP of DESm carried out at low temperatures and under solventless conditions holds promise for a sustainable framework for preparing biodegradable polymers for biomedical applications.

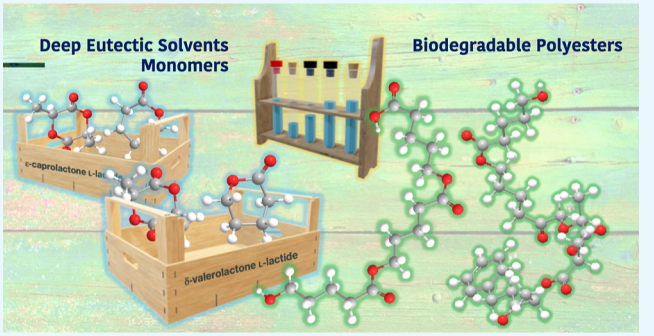

KEYWORDS: *ring opening polymerization, deep eutectic solvent monomers: valerolactone, lactide, polyesters*

1. INTRODUCTION

Poly(L-lactide) (PLLA) has been extensively studied in recent years due to its wide range of applications as the main component of polymeric materials in packing, pharmaceutical, and medical fields.[1] PLLA can be produced from renewable resources and stands out as a greener alternative to replace conventional petroleum-based polymers because of its biocompatibility and biodegradability. However, one of its main drawbacks is its brittleness, which limits its applications in areas where further processing and flexibility are needed. One strategy to improve its mechanical properties is to blend or copolymerize it with polyesters such as polylactones.[2−4]

Polylactones are biodegradable and biocompatible polyesters used in biomedicine and are usually obtained from monomers such as ε-caprolactone (CL), δ-valerolactone (VAL), δ-decalactone (DCL), and dodecalactone (DOCL).[2−4] Strategies for coupling the properties of PLLA with polycaprolactone (PCL) are currently the subject of intense research.[5,6] For instance, blending or copolymerizing PCL with PLLA to improve the strength and elongation properties of the resulting polymers without loss in biodegradability has been previously reported.[7]

PLLA and polylactones are predominantly synthesized through ring-opening polymerization (ROP) of lactide and lactones, respectively. Compared to other methods of polymerization, ROP allows higher molecular weights and lower dispersity of the polymers, which are essential characteristics that define their performance for specific applications. In addition to controlling its molecular weight, the degradation of PLLA can be tuned by modifying the aggregate structure, crystallinity, and external factors in the media, such as the pH or the use of enzymes.[8] PLLA and polylactones are industrially produced at high temperatures,[9−11] and organic solvents are used occasionally,[1] although polymerization in bulk is preferred for its economy and sustainability.[11] There has been deep concern with regard to the use of organic solvents because of their toxicity and negative environmental effects as many of them are volatile.[1,12] Similarly, tin metal catalysts approved by the FDA are typically used in PLLA and polylactone polymerization at high temperatures (above 120 °C),[10] offering an excellent control in designing complex

Received: March 23, 2023
Accepted: May 26, 2023
Published: June 23, 2023

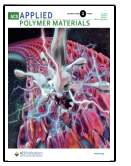

https://doi.org/10.1021/acsapm.3c00591
ACS Appl. Polym. Mater. 2023, 5, 5110−5121

Table 1. The Overall Conversion ($X_{overall}$) of PLLA−PY (Y = CL or VAL) and Molecular Weight (M_n) of the Polyester Obtained from ROP of LLA_{30}−CL_{70} and LLA_{30}−VAL_{70}

sample[a]	CAT	Temp. (°C)	[CAT:In] (mol ratio)	$X_{overall}$[b] (%)[c]	$M_{n,PLLA}$[c] (g mol^{-1})	$M_{n,PY}$[c] (g mol^{-1})
$PLLA_U$−PCL	DBU	37	1:1	91	2001	3402
$PLLA_N$−PCL	DBN	37	1:1	90	1879	3332
$PLLA_U$−PVAL-60	DBU	60	1:1	91	2257	5810
$PLLA_U$−PVAL	DBN	37	1:1	85	1850	3181
$PLLA_U$−PVAL-1	DBN	37	1:0.5	91	3848	4788
$PLLA_U$−PVAL-0	DBN	37	1:0.25	91	4951	4152
$PLLA_N$−PVAL	DBN	37	1:1	84	1757	3242

[a]ROP of LLA_{30}−VAL_{70} or LLA_{30}−CL_{70} DESm was carried out using MSA as the second organocatalyst and BnOH as the initiator (In). The molar ratio of [CAT:In] and [MSA] represented 5 and 3 wt % to DESm, respectively. In all the entries ROP was performed at 37 °C except for sample $PLLA_U$−PVAL-60. [b]Overall conversion was obtained by gravimetry. [c]M_n obtained by ^{1}H NMR.

architectures. However, recent regulations are limiting the use of metal-based catalysts, and because the purification of polymers can be arduous and can compromise the polymer performance in some areas, the use of organocatalysts stands as a viable alternative.[9,12,13]

In 2003, Abbott *et al.* reported a new family of solvents called deep eutectic solvents (DESs), comprising mixtures of organic molecules and salts with hydrogen bond-forming capabilities at eutectic compositions, *e.g.*, choline chloride and urea in a 1:2 molar ratio.[14] DESs have also attracted attention in polymer chemistry. For instance, due to their advantage of compositional plasticity, they can be used as solvents for polymerization as well as monomers that are part of the DES family.[15] The term deep eutectic solvent monomer (DESm) was introduced for systems where the eutectic mixture contains monomers that can undergo polymerization reactions and form polymers.[16] Thus, DESms are a new type of eutectic mixtures with polymerizable units.[5,17] In a pioneering work, Coulembier *et al.* reported the ROP of DESms based on mixtures of LLA and trimethylene carbonate (TMC) affording poly(LLA-*g*-TMC) gradient copolymers.[17] Similarly, a DESm based on LLA and CL was employed for producing blends of PLLA and PCL homopolymers.[5] The ROP in these two studies was carried out in the absence of organic solvents and using amidine-based organocatalysts.[5,12]

Utilizing a DESm as an all-in-one system (solvent and monomers) has proven to be a versatile and greener approach for polyester production at low temperature and under solventless conditions, either as homopolymer blends or as copolymers. In this work, we studied the thermal behavior of three novel DESm composed of LLA and different lactones such as VAL, *δ*-hexalactone (HEXL), and DCL at different molar ratios. The sequential ROP of the resulting DESm was studied using various organocatalysts such as 1,8-diazabicyclo [5.4.0] undec-7-ene (DBU), 5-diazabicyclo (4.3.0) non-5-ene (DBN), and methanesulfonic acid (MSA), and also benzyl alcohol (BnOH) as the initiator. Of the three DESms, only that formed by LLA−VAL yielded polyesters with high molecular weights. The obtained final product was PLLA and poly(*δ*-valerolactone) (PVAL) polymer blends, whose properties depended on the selection of the organocatalyst for LLA and the polymerization temperatures, including the controlled degradability under physiological conditions.

2. EXPERIMENTAL SECTION

2.1. Materials. VAL (≥97.5%), L-lactide (LLA, 98%), 1,8-diazabicyclo [5.4.0] undec-7-ene (DBU, 98%), 1,5-diazabicyclo (4.3.0) non-5-ene (DBN, 99%), methanesulfonic acid (MSA, 99.5%), benzyl alcohol (BnOH, 99%), DCL (≥99%), and deuterated chloroform ($CDCl_3$, 99.8 atom %) were obtained from Sigma-Aldrich. CL (97%) was obtained from Thermo Fisher Scientific. HEXL (>99.0%) was acquired from TCI Europe N.V. Absolute ethanol (EtOH, AR), methanol (MeOH, AR), and chloroform ($CHCl_3$, >98%) were purchased from Biosolve Chemicals. All materials were used without further purification.

2.2. Deep Eutectic Solvent Monomers Synthesis. The deep eutectic solvent monomers (DESm) were prepared by mixing LLA with CL, VAL, HEXL, or DCL at different molar ratios (*i.e.*, 20:80, 30:70, 40:60, and 50:50 LLA−lactone, respectively). The mixtures were heated at 90 °C until a clear homogeneous liquid was obtained. To make reference to LLA-lactone molar ratios, a subscript in each of the systems under study will be used, *e.g.*, LLA_{30}−CL_{70} for a DESm composed of 30 mol % LLA and 70 mol % CL.

2.3. ROPs of Deep Eutectic Solvent Monomers. The synthesis of polyesters was carried out by sequential ROP at 37 °C in bulk of DESm composed of LLA−CL, LLA−VAL, and LLA−HEXL at a 30:70 molar ratio. A solution of DBU or DBN (organocatalyst, [CAT] = 2.9 wt %) and BnOH (initiator, [In] = 2.1 wt %), with respect to DESm, in a proportion [CAT:In] = [1:1] mol %, was added to the DESm mixture with constant stirring. Subsequently, 3 wt % of MSA (co-organocatalyst) was added 1 min after starting the reaction. The obtained polyesters were named $PLLA_{CAT}$-*PY*, where CAT = U for DBU or N for DBN was assigned to the organocatalyst used for the LLA ROP, and *Y* corresponded to CL or VAL (see Table 1). Once the polymerization reached high conversions after 24 h, the polyesters obtained were purified by adding an ethanol excess at room temperature and washing each sample six to eight times to completely remove the residual monomers and oligomers. The recovered solids were dried at room temperature (RT) for 24 h. The overall conversion ($X_{overall}$) was determined by gravimetry and ^{1}H NMR. For the kinetics studies of DESm based on LLA−CL and LLA−VAL, the samples were prepared in individual vials and were terminated at different times, and the $X_{overall}$ was calculated by gravimetry. The general procedure was the same as described above. The final products were dissolved in chloroform and subsequently precipitated in cold methanol (−4 °C). The solution was then centrifuged at 4500 rpm for 10 min. Finally, the precipitated product was separated by decantation.

2.4. Characterization of DESm and Polyesters. ^{1}H NMR spectra were recorded at 600 MHz with a Varian VXR Spectrometer at RT using deuterium chloroform ($CDCl_3$).

Attenuated total reflection Fourier (ATR-FTIR) spectra were recorded on a Bruker VERTEX 70 spectrometer equipped with a platinum-ATR diamond single reflection accessory. The measurement resolution was 1 cm^{-1}, and the spectra were collected in the range of 4000−400 cm^{-1}.

Differential scanning calorimetry (DSC) measurements were carried out on a TA Instruments Q1000 DSC. The analysis of DESm and the polyesters obtained was performed on dry samples and with heating−cooling cycles. Scans for any DESm consisted of initial cooling from RT to −70 °C at a scan rate of 10 °C min^{-1} and keeping

https://doi.org/10.1021/acsapm.3c00591
ACS Appl. Polym. Mater. 2023, 5, 5110−5121

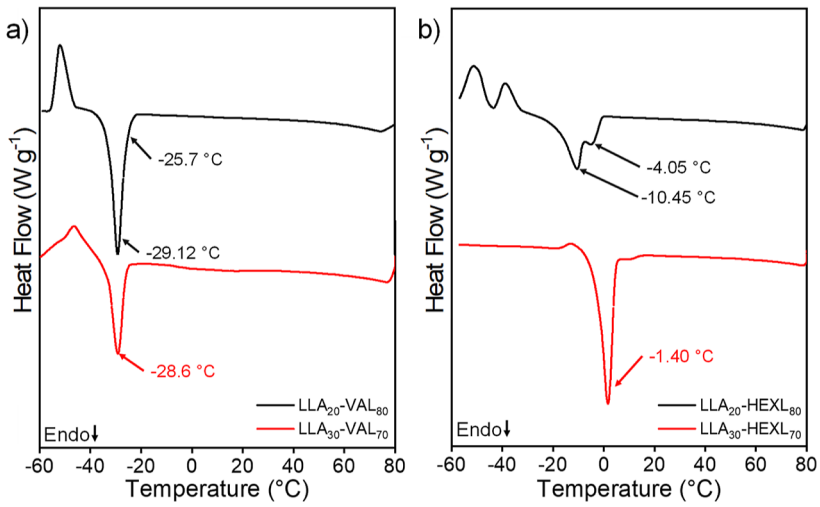

Figure 1. DSC scans for mixtures of (a) LLA−VAL and (b) LLA−HEXL at 20:80 and 30:70 molar ratios, respectively.

it at that temperature for 5 min; afterward, the temperature was increased to 90 °C and finally decreased again to RT at the same scan rate. The data were collected during heating run and the first scan. For the thermal properties of the polyesters, the analysis consisted of a similar initial cooling from RT to −70 °C, again at a scan rate of 10 °C min^{-1}, maintaining them at that temperature for 5 min, then increasing the temperature to 220 °C, and finally cooling to RT at the same scan rate.

The thermal stability and degradation behavior of the different samples were studied using thermogravimetric analysis (TGA) on a TA Instruments Discovery 5500 thermogravimetric analyzer by using an aluminum pan. Thermograms were recorded in the temperature range of 30−700 °C at a heating rate of 10 °C min^{-1} under a nitrogen atmosphere.

The X-ray diffraction (XRD) patterns of powdered samples were recorded on a Bruker D8 Advance diffractometer with Cu Kα radiation (λ = 0.1542 nm) in the angular range of 5−40° (2θ) at RT.

The molecular weight distributions (M_w/M_n) were determined by size exclusion chromatography (SEC) equipped with a triple detector: Viscotek Ralls detector, Viscotek Viscosimeter model H502, and Schambeck RI2912 refractive index detector. The separation was carried out by two PLgel 5μm MIXED-C and 300 mm columns from Agilent Technologies at 35 °C in THF (99% extra pure) stabilized with BHT as the eluent at a flow rate of 1.0 mL min^{-1}. The data acquisition was processed by using Viscotek Omnisec software version 5.0.

Diffusion order spectroscopy (DOSY) data were acquired using the pulse program *ledbpgp2s* installed in the topspin 3.6.2 software from Bruker with 95 gradient levels with a linear increase from 2 to 95% using a gradient of strengths up to 54 G/cm and 8 transients. The diffusion delay (Δ) was 150 ms, and the length of the square diffusion encoding gradient pulse (δ) was 0.6 ms. Laplace transformations for generating the diffusion dimensions were obtained with the Bruker Biospin Dynamics Center using a least-squares fitting routine with Monte Carlo error estimation analysis.

The contact angle was recorded by OCA20 (Data physics). The measurements were performed on films prepared by solvent casting. The obtained polyesters were dispersed in $CHCl_3$ and poured onto a glass plate, allowing the solvent to evaporate.

3. RESULTS AND DISCUSSION

3.1. Synthesis and Characterization of LLA−Lactone DESm. Deep eutectic solvent monomers (DESm) composed of mixtures of LLA and lactones, namely, VAL, HEXL, DCL, and CL (Figure S1 in the Supporting Information), were prepared in different molar ratios, 20:80, 30:70, 40:60, and 50:50 LLA−lactone, respectively, by heating the mixtures to 90 °C until transparent and homogeneous mixtures were obtained. The mixtures LLA_{30}−VAL_{70}, LLA_{30}−$HEXL_{70}$, and LLA_{30}−CL_{70} remained liquid upon cooling to RT. The rest of the samples with different molar ratios presented crystallization or were not homogeneous (Figure S1a−c in the Supporting Information). The thermal properties of the mixtures that remained stable and liquid at RT were further studied by DSC.

DSC scans of DESms composed of LLA and VAL (Figure 1a) show T_m = −28.6 °C and T_m = −29.1 °C for LLA_{30}−VAL_{70} and LLA_{20}−VAL_{80}, respectively. The observed melting points were lower than those of their pure constituents (T_m = −13 °C and T_m = 98.3 °C for VAL and LLA, respectively). However, in the 20:80 molar ratio, an additional melting point at T_m = −25.7 °C was observed, which indicates a different component or phase out of the eutectic composition, as reported for other mixtures near the eutectic point.[5,18]

The DSC results of LLA−HEXL mixtures are shown in Figure 1b, where a decrease in the melting point was observed for the LLA−HEXL DESm compared to the pure components. For the LLA_{30}−$HEXL_{70}$ mixture, only one melting point at T_m = −1.4 °C was detected, while for LLA_{20}−$HEXL_{80}$, two endothermic peaks appeared at T = −10.45 and −4.05 °C. These melting points are below the ones of their original constituents (HEXL T_m = 31 °C, and LLA T_m = 98.3 °C), which again indicates DESm formation. However, the presence of two thermal events in the 20:80 mixture suggests that this mixture is not completely homogeneous and that other phases or components are present in excess.[5,18] From the DSC scan of the LLA and DCL mixture, no thermal transition could be observed due to the absence of any melting point under the conditions assayed (Figure S2 in the Supporting Information). This can be explained by the steric hindrance and branching effects presented in the aliphatic moieties of DCL.

The LLA_{30}−VAL_{70} DESm was also analyzed by ^{1}H NMR spectroscopy once the presence of a single melting point was verified by DSC. The spectrum in Figure S3c in the Supporting Information, revealed that the peaks assigned to H_a (δ = 5.05 ppm) and H_b (δ = 1.70 ppm) corresponding to the methine proton [−C**H**−] and methyl group [−C**H**$_3$] of pure LLA shifted to 5.11 and 1.55 ppm, respectively, in the formed DESm of LLA_{30}−VAL_{70}. Similarly, shifts in the signals were observed in the mixture LLA_{30}−$HEXL_{70}$ (Figure S3e in the Supporting Information). These shifts confirm the formation

https://doi.org/10.1021/acsapm.3c00591
ACS Appl. Polym. Mater. 2023, 5, 5110−5121

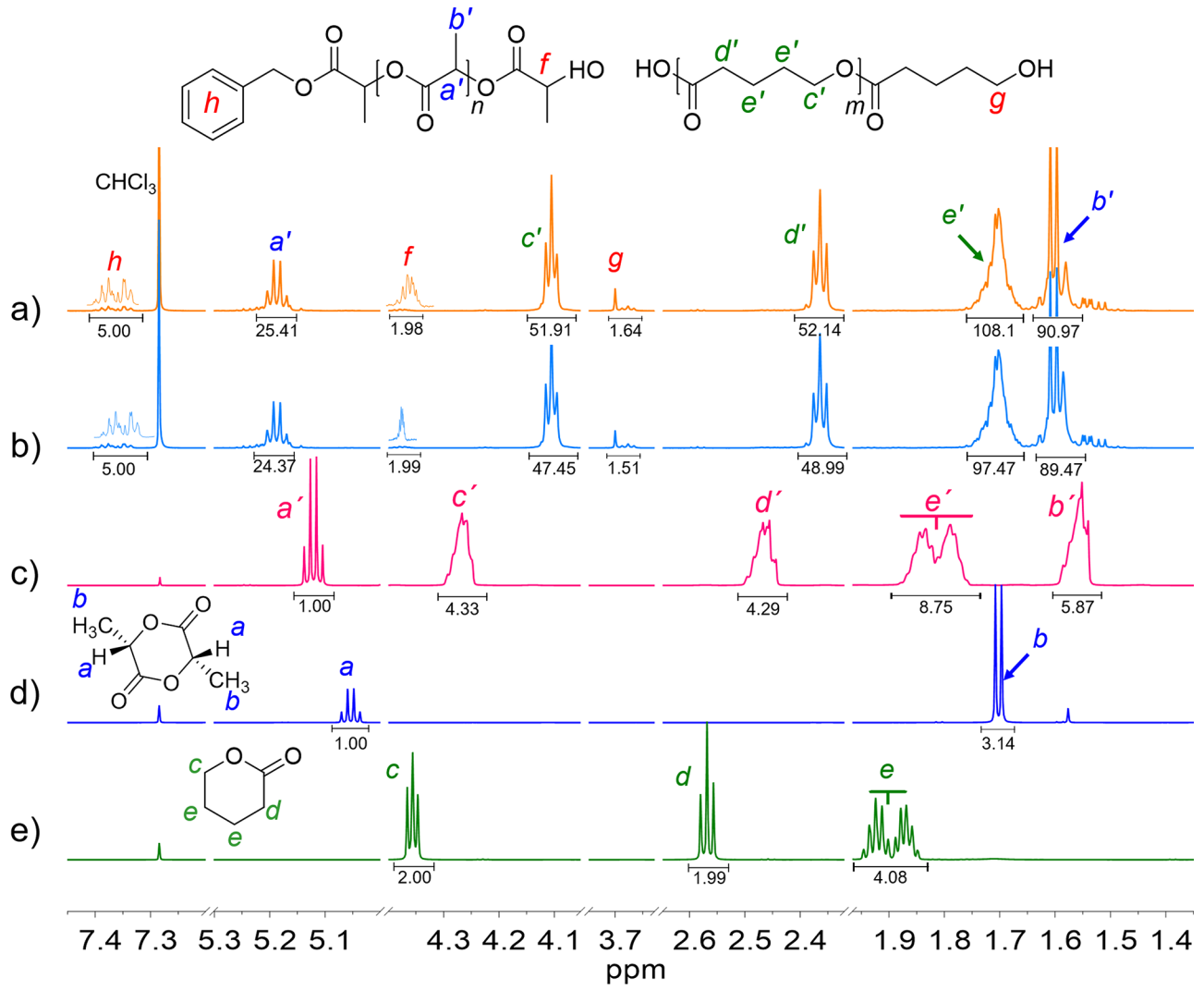

Figure 2. ^{1}H NMR spectra of the final product of the ROP of LLA_{30}–VAL_{70} at 37 °C using (a) DBU and (b) DBN as the organocatalysts of PLLA, (c) LLA_{30}–VAL_{70} DES mixture and the monomers (d) LLA, (e) VAL.

of the desired DESm, as reported previously by Pérez-García *et al.*, where similar peak shift behavior of LLA_{30}–CL_{70} DESm was observed.[5] For instance, the methylene proton [−C**H**$_2$−] (H_c) of pure VAL shifted from 4.36 to 4.27 ppm (Figure S3b,c in the Supporting Information), and the methine proton [−C**H**−] (H_l) and methyl group [−C**H**$_2$−] (H_i) of pure HEXL shifted from 4.46 to 4.36 ppm and 2.58 to 2.48 ppm, respectively (Figure S3d,e in the Supporting Information).

The LLA_{30}–VAL_{70} and LLA_{20}–VAL_{80} mixtures were also compared and studied by ^{1}H NMR analysis (Figure S4a in the Supporting Information). A larger shift in the signals of groups [−C**H**−] (H_a) and [−C**H**$_3$] (H_b) of LLA was observed in the ^{1}H NMR spectra of the mixture at a 30:70 molar ratio because it establishes stronger interactions with VAL in comparison to the 20:80 molar composition. This is further supported by the DSC results, where a single melting point was observed for the mixture with a 30:70 molar ratio, corresponding to the formation of the DESm (Figure 1a). However, for the corresponding LLA–DCL mixture, only the LLA methine at approximately 5.05 ppm slightly shifted (see Figure S4b in the Supporting Information).

To gain more understanding of the interactions between LLA and lactones, mixtures at a 30:70 molar ratio that presented a single melting point by DSC were studied by ATR-FTIR. These included mixtures of LLA–VAL and LLA–HEXL and the mixture of LLA–CL for comparison. In Figure S5 in the Supporting Information, the ATR-FTIR spectrum of LLA_{30}–VAL_{70} shows that the ester group peak of LLA shifted from 1756 to 1764 cm^{-1}, and for VAL, it shifted from 1722 to 1724 cm^{-1}, and the relative intensity of the carboxylic group [−**COO**−] increased in the DESm form. This behavior suggests the establishment of hydrogen bond interactions between the [−**COO**−] group of VAL and the protons of the [−C**H**− and −C**H**$_3$] groups from LLA, which also support the shifts observed by ^{1}H NMR.

The ATR-FTIR spectroscopy results of the other eutectic mixtures LLA_{30}–$HEXL_{70}$ and LLA_{30}–DCL_{70} were also studied. In Figure S5 in the Supporting Information, it is observed that the [−**COO**−] group of LLA shifted from 1756 to 1765 cm^{-1} when mixed with HEXL, and from 1751 to 1767 cm^{-1} when mixed with DCL (Figure S6a in the Supporting Information). However, the [−**COO**−] groups of HEXL and DCL at 1723 and 1728 cm^{-1}, respectively, did not show any shift in the mixtures, which points to weaker interactions with LLA in these mixtures. On the other hand, by comparing the relative intensity of the carbonyl group in HEXL and VAL

https://doi.org/10.1021/acsapm.3c00591
ACS Appl. Polym. Mater. 2023, 5, 5110−5121

when mixed with LLA in a 30:70 molar ratio, the increasing intensity when forming DESm was higher in VAL (Figure S6c in the Supporting Information). The change in the carbonyl vibrations of the DESm constituents confirms hydrogen bonding as the origin of the interactions that formed them, which in turn caused the depression in the melting points of DESm compared with the melting temperature of their individual components.[5]

3.2. Ring Opening Polymerization of LLA−DESm. LLA_{30}−VAL_{70} and LLA_{30}−$HEXL_{70}$ eutectic mixtures were selected as DESm for polymerization. We followed the methodology described in our previous work with the DESm of LLA−CL at the same molar ratio.[6] The overall reaction is depicted in Figure S7 in the Supporting Information. To ensure high conversions, the reaction was carried out for 24 h. Once the polymerization was completed, the purified products were studied by ^{1}H NMR spectroscopy. The $X_{overall}$ was determined gravimetrically by dividing the final mass of polymers by the theoretical mass expected from the complete polymerization of the corresponding monomers. For LLA−VAL DESm, the conversion was approximately 84%, and for LLA−HEXL mixture, the conversion obtained was *ca.* 30%. See Table 1.

The ROP of LLA in LLA−VAL DESm is selectively carried out when using DBU or DBN as the catalysts through a possible activation of both the alcohol and the monomer. Consequently, at the end of this stage, the PLLA chains were dispersed in the lactone, *i.e.*, VAL was released from the liquid DESm as the LLA was consumed during ROP. Subsequently, MSA, as the second organocatalyst, was added to the reaction mixture and catalyzed the ROP of the remaining VAL. In this second step, the hydroxyl groups of the previously formed lactidyl or residual water acted as initiators. Finally, PLLA−PVAL was obtained as the product. The rate of polymerization depended on the first catalyst used: DBU or DBN, as will be explained later.

Figure 2 shows a comparative ^{1}H NMR spectra of the LLA_{30}−VAL_{70} DESm and the polymers resulting from their ROP at 37 °C. The signals $H_{a'}$ (δ = 5.11 ppm) and $H_{b'}$ (δ = 1.55 ppm) corresponding to the methine [−C**H**−] and methyl group [−C**H$_3$**] of the LLA monomer in the DESm shifted in the ^{1}H NMR spectra of PLLA−PVAL (*i.e.*, $\delta_{Ha'}$ = 5.2 ppm and $\delta_{Hb'}$ = 1.60 ppm), and H_h and H_f denote the terminal aromatic group of BnOH (δ = 7.34 ppm) and the terminal methine (δ = 4.37 ppm), respectively, of PLLA. This confirms that the catalysts (DBU and DBN) selectively polymerized LLA in the DESm (Figure 2a,b). Furthermore, as a result of MSA catalyzing the second ROP of VAL, the peaks of H_c (δ = 4.26 ppm), H_d (δ = 2.56 ppm) and H_e (δ = 1.89 ppm) assigned to the [−C**H$_2$**−] groups in the ^{1}H NMR spectrum of VAL in the DESm also shifted in the ^{1}H NMR spectra of the final product (*i.e.*, $\delta_{Hc'}$ = 4.10 ppm, $\delta_{Hd'}$ = 2.36 ppm and $\delta_{He'}$ = 1.70 ppm). This confirms that MSA is a suitable organocatalyst for VAL ROP in the DESm. On the other hand, LLA−HEXL polymerization was carried out under the same conditions, but the signals corresponding to polymers were of very low intensity, corresponding to the low conversion obtained by gravimetry. Therefore, it was decided not to continue with the study of LLA−HEXL ROP (Figure S8 in the Supporting Information). This indicates that the ROP of HEXL is not efficiently catalyzed by MSA and could be explained by the steric effects of the methyl moiety in the HEXL structure compared with VAL. Hence, we will focus on the ROP of the LLA_{30}−VAL_{70} system, and a comparative study will be made with the previously reported LLA_{30}−CL_{70} system.[6]

As shown in Figure 2a,b, the ROP of LLA_{30}−VAL_{70} using DBU and DBN as catalysts of PLLA was confirmed by ^{1}H NMR analysis. However, different molecular weights calculated by NMR resulted from varying the initiator, being comparable to those reported in the literature.[19] The molecular weights (M_n) of PLLA and PVAL were calculated by Equations 1 and (2), where MW_{LLA} and MW_{VAL} are the molecular weights of LLA and VAL, respectively. M_n and $X_{overall}$ are listed in Table 1.

$$M_n(\text{gmol}^{-1}) = \frac{\int H_{a'}}{\int H_f}(\text{MW}_{\text{LLA}}) \quad (1)$$

$$M_n(\text{gmol}^{-1}) = \frac{\int H_{d'}}{\int H_g}(\text{MW}_{\text{VAL}}) \quad (2)$$

3.3. Kinetics Studies of ROP of LLA−CL and LLA−VAL at 37 °C by Varying the Catalyst. To better understand the sequential ROP of the LLA-forming DESm with VAL and CL, the ROP kinetics of LLA_{30}−VAL_{70} and LLA_{30}−CL_{70} were comparatively studied. The M_n and $X_{overall}$ of PLLA and PCL were calculated as described above.[6] The relationship between the conversion of LLA_{30}−CL_{70} DESm and the polymerization time is shown in Figure 3a, where it is observed that $X_{overall}$ is close to 90%, being slightly higher when DBU is used as a catalyst.

Figure 3b exhibits the semilogarithmic plot, $\ln([M]_0/[M])$ *versus* time, where $[M]_0$ and $[M]$ are the concentrations of monomers at the initial time (t = 0) and at any time, respectively, showing that the polymerization of LLA_{30}−CL_{70} follows three-stage kinetics, accounting for sequential polymerization. The first stage is observed almost instantaneously,

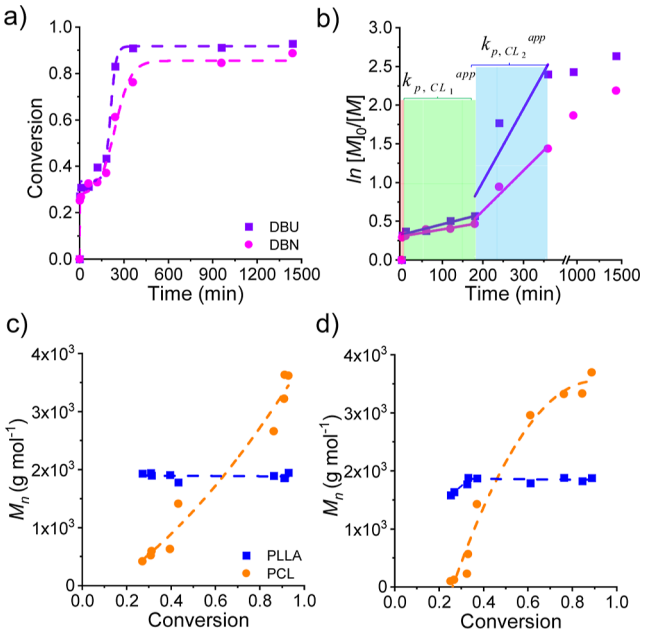

Figure 3. (a) Evolution of the conversion profiles, (b) linear fitting of eq 3 and dependence of M_n *versus* $X_{overall}$ using (c) DBU and (d) DBN as organocatalysts of PLLA for the sequential ROP of LLA_{30}−CL_{70} DESm at 37 °C. (Dashed lines denote tendencies, and solid lines are the linear regressions).

https://doi.org/10.1021/acsapm.3c00591
ACS Appl. Polym. Mater. 2023, 5, 5110−5121

reaching an $X_{overall}$ up to 25% in just 1 min of reaction, which is attributed to the rapid and complete polymerization of PLLA (30% molar ratio of the LLA−CL DESm) catalyzed by DBU or DBN, as reported previously.[20,21] The second stage encompassing the ROP of CL becomes slower, following *first-order* kinetics in an interval of 10−200 min, associated with the slope of the curve corresponding to the initiation rate constant (k_{p,CL_1}^{app}). This stage can be considered an induction period, representing the existence of structural rearrangement processes due to the initiator forming the active sites in a system having PLLA chains in the media after the addition of MSA, suggesting that rearrangement of the reacting species is required (*e.g.*, CL and MSA catalysts) before polymerization begins. Here, monomer molecules can access the active species without competition, which increases the rate of polymerization.[22]

In the third stage, the increase in viscosity in the reaction medium induces an abrupt increase in $X_{overall}$ in the system, where the propagation and termination steps become diffusion controlled. This scenario is consistent with what has already been reported in the literature and results in a change in the slope of the last stage corresponding to the propagation velocity constant (k_{p,CL_2}^{app}) of the PCL.[23,24] The values k_{p,CL_1}^{app} and k_{p,CL_2}^{app} can be determined with the other parameters associated with eq 3, where k_{p,Y_i}^{app} (Y = CL or VAL, i = 1 or 2) corresponds to the term $k_p[I]_0$. Notably, no segregation of the final polymers is observed. The results are shown in Table S1 in the Supporting Information.

$$\ln \frac{[M]_0}{[M]} = k_{p,Y_i}^{app} \times t \tag{3}$$

In the induction period of the second stage, it is evident that there is no significant difference in the value of k_{p,CL_1}^{app} using either DBU or DBN, as these catalysts affect only the ROP of LLA, which formed rapidly during the first stage. However, the difference emerges in the final stage of the CL propagation, since the value k_{p,CL_2}^{app} increases up to 4.5 times for the ROP where the previous LLA polymerization is catalyzed by DBU compared with the reaction catalyzed by DBN.

However, it is worth mentioning that these polymerizations were carried out under the same conditions of $[DESm]_0$:$[CAT]_0$:$[In]_0$, only changing the nature of the catalyst for LLA (DBU or DBN) and adding to both MSA as the catalyst for the ROP of CL. Therefore, the increase in k_{p,CL_2}^{app} when DBU is used with respect to DBN is likely due to the type of polymers obtained at the end, a blend of homopolymers or a block copolymer, as follows.

It was reported that the choice of organocatalyst for the ROP of the LLA_{30}−CL_{70} DESm at 37 °C is decisive to obtain a blend of PLLA and PCL homopolymers in the case of DBU or a PLLA−PCL block copolymer in the case of DBN.[6] In the former case, PCL chains initiate with residual water and propagate independently of PLLA already formed, producing a blend of PLLA and PCL homopolymers. Conversely, in the latter case, PLLA chains serve as the macroinitiator of CL, yielding block copolymers with slower kinetics.

Figure 3c,d depicts the evolution of M_n *versus* $X_{overall}$ in LLA_{30}−CL_{70} polymerization. As mentioned above, it is evident that the polymerization of PLLA in the first reaction is achieved faster, almost immediately reaching $M_n \approx 2000$ g mol^{-1} with an $X_{overall}$ = 25% and remaining constant throughout the reaction when DBU is used as catalyst. When using DBN, the $X_{overall}$ of PLLA increases discreetly linearly between 20 and 25% of M_n until reaching 2000 g mol^{-1}, remaining constant throughout the conversion profile (Figure 3d). The M_n of PCL increases with respect to $X_{overall}$ of the system, indicating the growth of the polymer chain, continuously forming PCL and reaching a $M_n \approx 3000$ g mol^{-1}, irrespective of the organocatalyst employed for the ROP of LLA. However, some kinetics differences are noticed in both cases, attributed to the formation of blends of homopolymers or block copolymers, as discussed above.

Kinetics studies of the ROP of LLA_{30}−VAL_{70} were also carried out under the same conditions as those used for LLA_{30}−CL_{70}. The $X_{overall}$ of monomers was monitored by gravimetry, and Figure 4a shows that the conversion reached

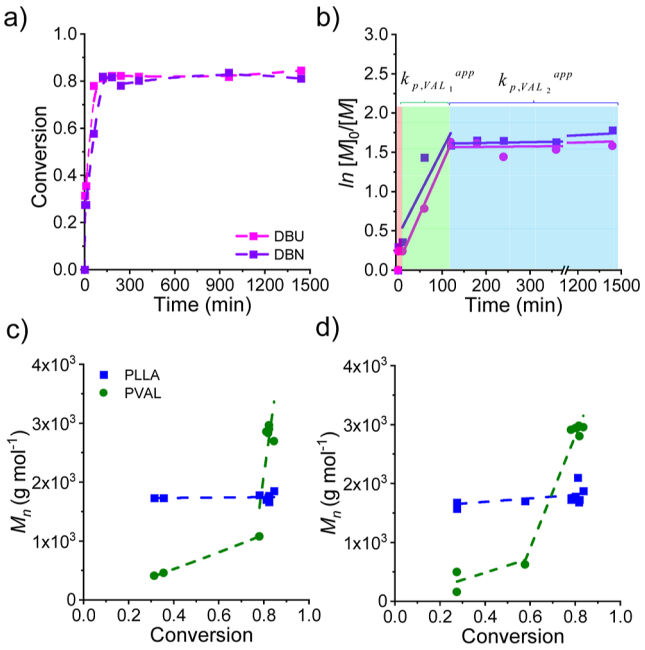

Figure 4. (a) Evolution of the conversion profiles, (b) linear fitting of eq 3 and dependence of M_n *versus* $X_{overall}$ using (c) DBU and (d) DBN as organocatalysts of PLLA for the sequential ROP of LLA_{30}−VAL_{70} DESm at 37 °C. (Dashed lines denote tendencies, and solid lines are the linear regressions).

approximately 80%; however, no significant difference in their behavior was observed when using DBU or DBN as the catalyst. Table S1 in the Supporting Information shows the values of k_{p,VAL_1}^{app} and k_{p,VAL_2}^{app} during the sequential ROP of LLA_{30}−VAL_{70}. These were obtained by adjusting the *first-order* kinetic data according to eq 3 in an interval of 10−150 min (k_{p,VAL_1}^{app}), *i.e.*, after the first ROP of LLA is completed. Figure 4b shows that the polymerization is inhibited during the rest of the reaction after 150 min, since the evolution of the polymerization rate presents a constant behavior and the estimated values for k_{p,VAL_2}^{app} are extremely small, irrespective of using DBU or DBN as the catalyst (on the order of 10^{-6} s^{-1}); the opposite behavior is observed when performing the ROP of LLA_{30}−CL_{70} under the same conditions. In addition, a comparative study of Figures 4b and 3b confirms that the polymerization of LLA_{30}−VAL_{70} is much faster than that of

https://doi.org/10.1021/acsapm.3c00591
ACS Appl. Polym. Mater. 2023, 5, 5110−5121

LLA_{30}−CL_{70}. This is in agreement with the results reported in the literature about these ROP reactions in solution.[13,25−27]

In Figure 4c,d, the evolution of M_n in the LLA_{30}−VAL_{70} conversion was followed, varying the type of catalyst for the ROP of LLA, observing that in both systems, LLA reached $X_{overall}$ = 30%, generating initial PLLA chains embedded in liquid VAL.

However, VAL, unlike CL, is added in low proportions under a linear behavior in conversions from 30 to 80%, when DBU is used as the catalyst, and up to 60% when DBN is used. At conversions higher than 60%, the viscosity of the medium increases, thus favoring the polymerization of VAL, reaching $M_n \approx 3000$ g mol^{-1}.

3.4. Thermal Properties and Crystallinity of PLLA−PCL and PLLA−PVAL. The mole fraction of monomers (F_{PLLA}:F_Y, Y = CL or VAL) in the polymers resulting from the ROP of LLA_{30}−CL_{70} and LLA_{30}−VAL_{70} was determined from the ^{1}H NMR spectra after removal of oligomers and residual monomers by the purification step. The mole fraction (F_{PLLA}:F_Y) of the homopolymer composition of PLLA−PCL and PLLA−PVAL at the end of the polymerization, 47:53 and 45:55, respectively, differed with respect to the initial molar composition (f_{LLA}:f_Y), 30:70 LLA-lactone. This means that the oligomers of PVAL or PCL and the residual monomers of VAL and CL were removed from the final product during the purification process. Figure S9 in the Supporting Information shows the SEC results and the elution of the $PLLA_U$−PCL sample before and after the purification step. The first bimodal peak at low retention volume corresponds to the PCL and PLLA blend, while the peak at higher retention volume corresponded to PCL oligomers. The decreased intensity of the oligomer peak after purification indicates the successful removal of oligomers.

The thermal properties of the obtained polyesters were studied by DSC. Figure S10 shows the thermograms for the samples listed in Table 2. The first endothermic peaks at 61 and 57 °C correspond to the melting point (T_m) of PCL (T_m = 62 °C)[28] and PVAL (T_m = 58 °C),[29] and the second endothermal peaks corresponded to the T_m of PLLA, which was found between 122.2 and 133.5 °C. The crystallinity (X_c) of the final polyester was calculated by eq 4.

Table 2. Mole Fraction of Polymers (F_Y, Y = PCL or PVAL) and Thermal Properties of the Polyester Obtained From the ROP of LLA_{30}−CL_{70} and LLA_{30}−VAL_{70}

sample[a]	[CAT:In] (mol ratio)	F_{PLLA}:F_Y[b] (mol %)	$T_{m,PLLA}$[c] (°C)	$T_{m,Y}$[c] (°C)	$X_{c,PLLA}$[c] (%)	$X_{c,Y}$[c] (%)
$PLLA_U$−PCL	1:1	45:55	133	61	35	73
$PLLA_N$−PCL	1:1	45:55	125	61	38	73
$PLLA_U$−PVAL-60	1:1	46:54	127	56	36	35
$PLLA_U$−PVAL	1:1	47:53	131	57	34	69
$PLLA_U$−PVAL-1	1:0.5	47:53	121	56	39	47
$PLLA_U$−PVAL-0	1:0.25	47:53	128	60	36	50
$PLLA_N$−PVAL	1:1	47:53	122	56	44	70

[a]ROP of LLA_{30}−VAL_{70} or LLA_{30}−CL_{70} DESm was carried out using MSA as the second organocatalyst and BnOH as the initiator. The molar ratio of [CAT:In] and [MSA] represented 5 and 3 wt % to the DESm, respectively. In all the entries, ROP was performed at 37 °C, except for sample $PLLA_U$−PVAL-60. [b]The mole fraction of the monomers (F_{PLLA}:F_Y) was obtained by ^{1}H NMR. [c]Thermal properties calculated by DSC.

$$X_c = \frac{100}{x^a}\left(\frac{\Delta H_m^a}{\Delta H_0}\right) \quad (4)$$

where X_c and x^a denote the degree of crystallinity and mass fraction of component a, respectively, in the DESm. ΔH_m^a and ΔH_{m_0} correspond to the experimental melting enthalpy of component a (obtained by DSC) and the theoretical value with 100% crystallinity ($\Delta H_{m_0,PVAL}$ = 182 J mol^{-1}, $\Delta H_{m_0,PCL}$ = 135.44 J mol^{-1}, and $\Delta H_{m_0,PLLA}$ = 106 J mol^{-1}, respectively).[5,30]

The T_m and X_c of the PLLA−PVAL and PLLA−PCL in the polymer varying the DBU or DBN as catalyst are shown in Figure 5. It is important to mention that regardless of the type of catalyst used, DBU or DBN, there is no significant difference when comparing the T_m values for the final polyesters (Figure 5, blue and purple solid and dotted bars).

These obtained polyesters presented semicrystalline behavior, as observed by XRD, showing the characteristic peaks of PLLA at 2θ values of 16 and 19°, of PCL at 21.4 and 23.8°, and of PVL at 21.7 and 24.11° (Figure S11 in the Supporting Information).[31]

Figure 5 shows that the crystallinity of the resulting PLLA is slightly favored when using DBN for the ROP of LLA_{30}−CL_{70} (Figure 5a), which is greater for the ROP of LLA_{30}−VAL_{70}. As discussed previously, although the polymerization of LLA in both systems ($PLLA_U$−PCL and $PLLA_N$−PCL) reached complete conversions within minutes, slightly lower kinetics in the case of DBN may have allowed the rearrangement of PLLA chains and thus increased its crystallinity (see Figure 3d). PCL and PVAL exhibit higher crystallinity than PLLA. Furthermore, the lower rate of polymerization of CL compared to that of VAL in the mixtures with LLA did not significantly affect the crystallinity of the corresponding PCL and PVAL ($X_c \approx$ 73% and X_c = 70%, respectively).

The T_m of PLLA of all samples are significantly lower than the T_m of PLLA synthesized *via* conventional methods ($T_m \approx$ 176 °C);[32] this could be associated with a diluent effect of PVAL or PCL embedded in the crystalline regions of PLLA, either as blends or forming block copolymers, thus resulting in materials with lower T_m. In general, PVAL has a lower melting point than PCL, and as expected, PVAL polymerized in the presence of PLLA also exhibits a lower T_m than PCL polymerized under similar conditions.[33] Similarly, PLLA synthesized using DBN as the organocatalyst and $PLLA_N$−PCL or $PLLA_N$−PVAL possess a lower T_m compared with those obtained with DBU.

The effect of the variation in the molar ratio of BnOH and the reaction temperature on the thermal properties and crystallinity of the final products is shown in Figure S12 in the Supporting Information. The T_m of $PLLA_U$ and PVAL remained nearly unchanged when decreasing the molar ratio of initiator (1 to 0.25) (Figure S12a in the Supporting Information), being *ca.* 130 and 57 °C, respectively. However, the molar ratio of BnOH with respect to DBU has a direct impact on the X_c of PVAL, for instance, reaching a maximum of 69% at higher concentrations. This corresponds to the fact

https://doi.org/10.1021/acsapm.3c00591
ACS Appl. Polym. Mater. 2023, 5, 5110−5121

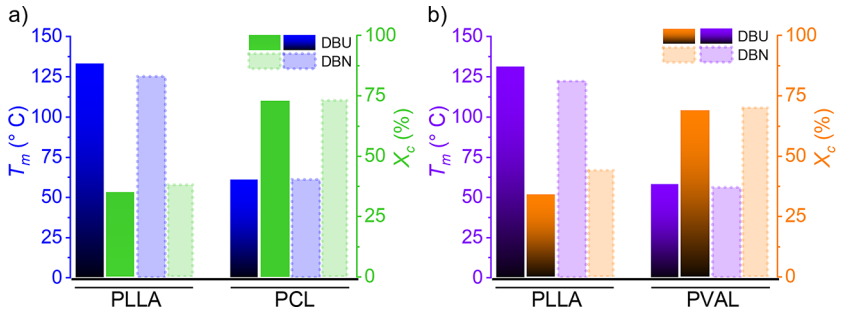

Figure 5. Melting point (T_m, blue and purple bars) and crystallinity (X_c, green and orange bars) of (a) PLLA−PCL and (b) PLLA−PVAL in the polymer blends varying the use of DBU (solid line bars) or DBN (dashed lines bars) as the catalyst.

that M_n of PLLA is *ca.* 1850 g mol^{-1} with a higher proportion of initiator, which allows the polymeric chains with low M_n to form crystalline domains more easily.

On the other hand, Figure S12b in the Supporting Information shows that the increasing of the reaction temperature from 37 to 60 °C does not have a noticeable effect on the T_m and X_c of PLLA$_U$, both remaining unchanged (T_m = 128 °C and X_c = 35), while for PVAL, the X_c is higher when the ROP is carried out at 37 °C. These results agree with the M_n values of polyesters obtained at the same temperatures (Figure S13 in the Supporting Information), being lower at 60 °C than at 37 °C, since lower temperature allow the polymeric chains to better reorganize into highly crystalline domains.

3.5. Polymer Architecture. To obtain deeper insights into the final product composition, PLLA$_U$−PVAL and PLLA$_N$−PVAL were analyzed by ^{1}H NMR DOSY. Figure 6a shows a broad distribution of coefficients in the DOSY spectrum of polyester PLLA$_U$−PVAL. The higher diffusion coefficient corresponded to heavier species, consistent with PVAL, and the lower diffusion coefficient corresponded to PLLA. The signals of each species were compared with the upper axis representing the corresponding ^{1}H NMR spectrum. These results show that the M_n of PVAL was higher than that of PLLA, as observed by the M_n calculation obtained from ^{1}H NMR (see Table 1 and Figure 6). Additionally, the signals of terminal OH-containing groups [−C**H**−] (H_f) and [−C**H$_2$**−] (H_g) identified in the ^{1}H NMR spectra of PLLA$_{CAT}$−PVAL, do not show any changes in their chemical shift or in their intensity along the ROP (Figure 2), which confirmed that both PLLA and PVAL exist as independent homopolymers in a polymer blend.

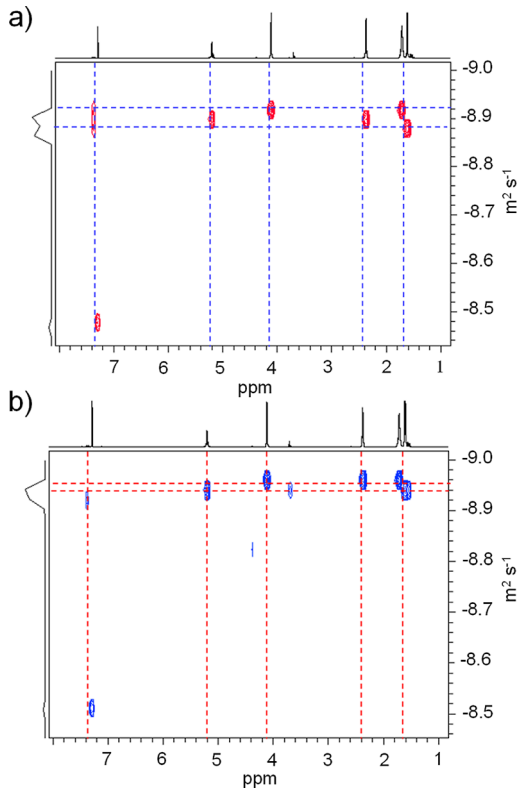

Figure 6. DOSY spectra of (a) PLLA$_U$−PVAL and (b) PLLA$_N$−PVAL in $CDCl_3$. The diffusion coefficient D_M (cm^2/s) is indicated for each component.

Conversely, in the case of sample PLLA$_N$−PVAL (Figure 6b), a narrower set of diffusion coefficients were observed, which can be mainly attributed to the presence of a block copolymer of poly(LLA-*b*-VAL), but other species cannot be ruled out. These results suggest the successful synthesis of poly(LLA-*b*-VAL) from the ROP of VAL-based DESm, where the initial hydroxyl-terminated PLLA homopolymer acts as the macroinitiator for the subsequent ROP of VAL catalyzed by MSA. Nevertheless, compared with the results of poly(LLA-*b*−CL),[6] here, the distribution of the diffusion coefficients, as shown in Figure 6b, is broad and presents a small shoulder. This is consistent with a polymer mixture of block copolymers and homopolymers, as the presence of the terminal H_f in the ^{1}H NMR of PLLA suggests in Figure 2.

Size-exclusion chromatography (SEC) measurements were conducted to analyze the polyesters listed in Table 1. Figure 7a shows bimodal peaks at low elution times (13−16 min), in PLLA$_U$−PCL and PLLA$_N$−PCL, corresponding to PCL with a higher molecular weight and PLLA with a lower molecular weight. Similarly, peaks of PVAL and PLLA are observed in PLLA$_U$−PVAL and PLLA$_N$−PVAL. These results are in line with the M_n obtained by ^{1}H NMR spectroscopy (Table 1). It is important to mention that the distribution of peaks is independent of the polymer architecture (homopolymers and block copolymers), and the differences between M_n and M_w were attributed to the change in the hydrodynamic volume.

To demonstrate the differences in samples mainly composed of homopolymers or block copolymers, a solubility test of the polyesters PLLA$_U$−PVAL and PLLA$_N$−PVAL was performed in THF at −4 °C, with a concentration of the polyesters of 0.55 g mL^{-1}. The insolubility of PLLA in THF under cold conditions was considerably improved with the PVAL counterpart presented in sample PLLA$_N$−PVAL, which contains block-copolymers. Therefore, a stable and clear

https://doi.org/10.1021/acsapm.3c00591
ACS Appl. Polym. Mater. 2023, 5, 5110−5121

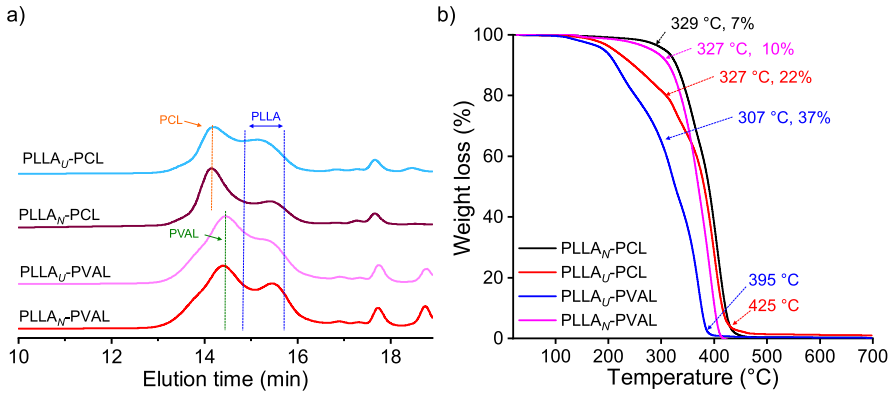

Figure 7. (a) SEC scans and (b) TGA curves of the final product of the ROP of LLA_{30}−CL_{70} and LLA_{30}−VAL_{70} at 37 °C using DBN and DBU as the organocatalysts of PLLA.

solution was observed. Conversely, the scant solubility of $PLLA_U$ in $PLLA_U$−PVAL led to gelled solutions in THF at −4 °C (see Figure S14 in the Supporting Information), as direct consequence of the presence of individual homopolymers (*i.e.*, PLLA and PVAL) in the polyester, forming a heterogeneous mixture.

3.6. Thermal Stability. The thermal stability and thermal degradation of the polyesters were studied by TGA. The $PLLA_U$−PCL and $PLLA_U$−PVAL samples, mainly composed of homopolymer blends, showed two thermal degradation (T_d) steps. The first degradation occurred at $T_d \approx 327$ °C and $T_d \approx 307$ °C with mass losses of approximately *ca.* 22 and 37%, for the polymers containing PCL and PVAL, respectively. They were attributed to PLLA degradation (with a previously reported T_d of about 365 °C),[34] with PLLA being approximately 30 mol % of the final composition of the polymer blend. The second step of degradation occurred between $T_d \approx 395$−425 °C, temperatures at which decomposition of PVAL and PCL occur in accordance with the values reported, and $T_d \approx 410$ and 520 °C.[29,34] This evidence indicates that $PLLA_U$−PVAL and $PLLA_U$−PCL were composed of blends of homopolymers. Conversely, the samples polymerized with DBN ($PLLA_N$−PCL and $PLLA_N$−PVAL) showed one main step of degradation denoting higher thermostability. At temperatures of approximately 330 °C, mass losses of 7 and 10% occurred in $PLLA_N$−PCL and $PLLA_N$−PVAL, respectively, which are lower than those in the $PLLA_U$−PCL and $PLLA_U$−PVAL samples due to the presence of block copolymers (Figure 7b).

3.7. Degradability Test and Contact Angle. The design of polyesters with rapid and controllable degradation can benefit from polyesters with low M_n, between 2000 and 3000 g mol^{-1}, such as those in this work obtained from the ROP of DESm at 37 °C. These polymerizations were carried out at a low temperature, excluding metal catalysts and organic solvents, opening the possibility for applications in biomedical areas owing to the green character of the synthesis. Degradation of polyesters such as PLLA and PVAL occurs through two stages by surface or bulk degradation mechanisms and is autocatalyzed by acidic by-products that are produced by chain hydrolytic incision.[35]

Parameters such as crystallinity, molecular weight, and molecular architecture all play important roles in the degradation performance, where water diffusion is restricted in highly crystalline polyesters, thus decreasing the degradation rate.[35] Figure 8a shows the mass loss degradation profile for

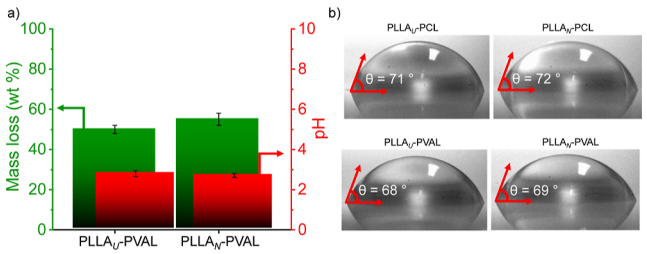

Figure 8. (a) Mass loss (wt %) profile degradation of the samples after 28 days at 37 °C and (b) water contact angle of the final product of the ROP of LLA_{30}−CL_{70} and LLA_{30}−VAL_{70} at 37 °C using DBN and DBU as the organocatalysts of PLLA.

$PLLA_U$−PVAL and $PLLA_N$−PVAL in phosphate buffer solution with pH = 7.4 at 37 °C, the mass losses after 28 days being *ca.* 50 and 55%, respectively. The higher crystallinity of $PLLA_N$−PVAL resulted in a lower mass loss. Early degradation was reported to take place on the surface,[35] as could be observed in the $PLLA_N$−PVAL sample in Figure S15 in the Supporting Information, where after 28 days, the diameter decreased, as did the pH of the solution from 7.4 to 2.8 due to the acidic nature of the released by-products of degradation. The degradation characteristics of polyesters could be applied in areas that require short-term degradation profiles in acidic media, such as drug delivery systems or the release of special cargos in the agroindustry.[31,33,36−39]

Figure 8b shows the water contact angle of the polyesters obtained from ROP of LLA_{30}−VAL_{70} at 37 °C using DBN and DBU compared with their counterparts having PCL (LLA_{30}−CL_{70}). The contact angle was approximately 70° in all the samples, *i.e.*, slightly hydrophobic, as expected.[38,40−42] The water contact angle obtained for the $PLLA_U$−PCL sample was 71°, and for $PLLA_U$−PVAL, it was 68°. A slightly decreased contact angle indicates reduced hydrophobicity, in agreement with data reported for PVAL, being comparatively less hydrophobic than PLLA−PCL.[37] In general, hydrophobicity decreases the water permeability in both polycaprolactone and polyvalerolactone, which reduces degradation by erosion.

4. CONCLUSIONS

In this work, we successfully obtained binary DESm composed of LLA with lactones, such as VAL and HEXL, at a 30:70 molar ratio. Sequential ROP of the DESm at low temperatures under solventless conditions involved two steps. In the first step, the organocatalyst (DBU or DBN) allowed the ROP of

https://doi.org/10.1021/acsapm.3c00591
ACS Appl. Polym. Mater. 2023, 5, 5110−5121

LLA contained in the DESm, with BnOH as the initiator. In the second step, lactone ROP (VAL or HEXL) was carried out by adding a second organocatalyst (MSA). Notably, a high conversion (*ca.* 80%) was only reached in the ROP of the LLA and VAL mixture, resulting in homopolymers and copolymer blends composed of PLLA and PVAL with high crystallinity.

The kinetics of the ROP of the LLA_{30}–VAL_{70} DESm comprise three stages; the first stage is attributed to the almost instantaneous polymerization of LLA, while the second and third stages include the induction and propagation periods of VAL, respectively. Contrary to the polymerization rate of LLA in CL, different amidine organocatalysts (DBU or DBN) did not affect the VAL rate in the LLA_{30}–VAL_{70} DESm, and both reached similar rates M_n. Nevertheless, properties such as thermal stability, diffusion coefficients of the polymeric species (by DOSY NMR), or solubility differed in the final polyesters, which reflects the different architectures achieved, *e.g.*, mainly block copolymers in the case of $PLLA_N$–PVAL or homopolymer blends in $PLLA_U$–PVAL. These results point to a major effect of the organocatalyst employed for LLA polymerization, proving decisive for the final architecture of subsequent ROP of VAL, either PLLA functioning as a macroinitiator for PVAL blocks or as a mere spectator of the VAL ROP.

The thermal properties and crystallinity of $PLLA_N$–PVAL and $PLLA_U$–PVAL are in accordance with their overall architecture, with $PLLA_N$ T_m higher than $PLLA_U$, and in the case of PVAL, M_n and X_c remain unchanged, either when there is $PLLA_N$ or $PLLA_U$ in the second stage of polymerization. The effect of the initiator concentration on the M_n of PLLA was as expected in the LLA_{30}–VAL_{70} DESm, *i.e.*, the lower the initiator, the higher the M_n. On the other hand, the increase in the ROP temperature led to lower crystallinity on PVAL and higher M_n in both PLLA and PVAL.

In summary, the ROP of DESm composed of LLA and VAL was carried out excluding metal catalysts and organic solvents under mild temperature conditions and unsophisticated atmospheres, thereby underscoring the green credentials of the processes. These findings pave the way for the design of polyesters with rapid and controllable degradation, potentially applicable to biomedical devices.

■ ASSOCIATED CONTENT

Supporting Information

The Supporting Information is available free of charge at https://pubs.acs.org/doi/10.1021/acsapm.3c00591.

Chemical structures, DSC scans, ^{1}H NMR and ATR-FTIR spectra of LLA and lactones and their mixtures (DESm) used in this study, DSC scans, ^{1}H NMR, ATR-FTIR, SEC traces, XRD scans, thermal properties, M_n, solubility test, and degradation profile of the polymer blends obtained by the ROP (PDF)

■ AUTHOR INFORMATION

Corresponding Authors

Katja Loos − *Macromolecular Chemistry and New Polymeric Materials, Zernike Institute for Advanced Materials, University of Groningen, 9747AG Groningen, The Netherlands;* orcid.org/0000-0002-4613-1159; Email: k.u.loos@rug.nl

Josué D. Mota-Morales − *Centro de Física Aplicada y Tecnología Avanzada (CFATA), Universidad Nacional Autónoma de México (UNAM), Querétaro, QRO 76230, Mexico;* orcid.org/0000-0001-8257-0709; Email: jmota@fata.unam.mx

Authors

Martín Castillo-Santillan − *Centro de Física Aplicada y Tecnología Avanzada (CFATA), Universidad Nacional Autónoma de México (UNAM), Querétaro, QRO 76230, Mexico; Macromolecular Chemistry and New Polymeric Materials, Zernike Institute for Advanced Materials, University of Groningen, 9747AG Groningen, The Netherlands*

Dina Maniar − *Macromolecular Chemistry and New Polymeric Materials, Zernike Institute for Advanced Materials, University of Groningen, 9747AG Groningen, The Netherlands*

María C. Gutiérrez − *Instituto de Ciencia de Materiales de Madrid (ICMM), Consejo Superior de Investigaciones Científicas (CSIC), Madrid 28049, Spain;* orcid.org/0000-0001-8612-7974

Priscila Quiñonez-Angulo − *Centro de Física Aplicada y Tecnología Avanzada (CFATA), Universidad Nacional Autónoma de México (UNAM), Querétaro, QRO 76230, Mexico;* orcid.org/0000-0001-6376-5199

José Román Torres-Lubian − *Centro de Investigación en Química Aplicada (CIQA), Saltillo, Coahuila 25294, Mexico*

Complete contact information is available at: https://pubs.acs.org/10.1021/acsapm.3c00591

Notes

The authors declare no competing financial interest.

■ ACKNOWLEDGMENTS

The authors gratefully acknowledge the financial support received from PAPIIT-UNAM through grant IA206022, the Zernike Institute for Advanced Materials, and the University of Groningen (UG). They also thank Jur van Dijken (UG-Zernike) for the technical assistance provided in acquiring DSC and TGA thermograms, Albert J. J. Woortman (UG-Zernike) for obtaining GPC chromatograms, Pieter van der Meulen for obtaining DOSY spectra, and Guillermo Vazquez (CFATA-UNAM). Priscila Quiñonez-Angulo acknowledges the support provided for this research through a post-doctoral fellowship from the National Council of Science and Technology (CONACYT) of Mexico.

■ REFERENCES

(1) Castro-Aguirre, E.; Iñiguez-Franco, F.; Samsudin, H.; Fang, X.; Auras, R. Poly(Lactic Acid)—Mass Production, Processing, Industrial Applications, and End of Life. *Adv. Drug Delivery Rev.* **2016**, *107*, 333−366.

(2) Hamad, K.; Kaseem, M.; Yang, H. W.; Deri, F.; Ko, Y. G. Properties and Medical Applications of Polylactic Acid: A Review. *eXPRESS Polym. Lett.* **2015**, *9*, 435−455.

(3) Li, F. J.; Zhang, S. D.; Liang, J. Z.; Wang, J. Z. Effect of Polyethylene Glycol on the Crystallization and Impact Properties of Polylactide-Based Blends. *Polym. Adv. Technol.* **2015**, *26*, 465−475.

(4) Sangroniz, A.; Sangroniz, L.; Hamzehlou, S.; Aranburu, N.; Sardon, H.; Sarasua, J. R.; Iriarte, M.; Leiza, J. R.; Etxeberria, A. Lactide-Valerolactone Copolymers for Packaging Applications. *Polymers* **2021**, *14*, 52.

(5) Pérez-García, M. G.; Gutiérrez, M. C.; Mota-Morales, J. D.; Luna-Bárcenas, G.; Del Monte, F. Synthesis of Biodegradable Macroporous Poly(L-Lactide)/Poly(ϵ-Caprolactone) Blend Using

Oil-in-Eutectic-Mixture High-Internal-Phase Emulsions as Template. *ACS Appl. Mater. Interfaces* **2016**, *8*, 16939−16949.
(6) Castillo-Santillan, M.; Torres-Lubian, J. R.; Martínez-Richa, A.; Huerta-Marcial, S. T.; Gutierrez, M. C.; Loos, K.; Peréz-García, M. G.; Mota-Morales, J. D. From Polymer Blends to a Block Copolymer: Ring-Opening Polymerization of L-Lactide/ε-Caprolactone Eutectic System. *Polymer* **2022**, *262*, 125432.
(7) Yang, X.; Liu, S.; Yu, E.; Wei, Z. Toughening of Poly(l -Lactide) with Branched Polycaprolactone: Effect of Chain Length. *ACS Omega* **2020**, *5*, 29284−29291.
(8) Sherck, N. J.; Kim, H. C.; Won, Y. Y. Elucidating a Unified Mechanistic Scheme for the DBU-Catalyzed Ring-Opening Polymerization of Lactide to Poly(lactic acid). *Macromolecules* **2016**, *49*, 4699−4713.
(9) Basterretxea, A.; Gabirondo, E.; Jehanno, C.; Zhu, H.; Coulembier, O.; Mecerreyes, D.; Sardon, H. Stereoretention in the Bulk ROP of l -Lactide Guided by a Thermally Stable Organocatalyst. *Macromolecules* **2021**, *54*, 6214−6225.
(10) Basterretxea, A.; Jehanno, C.; Mecerreyes, D.; Sardon, H. Dual Organocatalysts Based on Ionic Mixtures of Acids and Bases: A Step Toward High Temperature Polymerizations. *ACS Macro Lett.* **2019**, *8*, 1055−1062.
(11) Chen, Y.; Zhang, J.; Xiao, W.; Chen, A.; Dong, Z.; Xu, J.; Xu, W.; Lei, C. Reinvestigation of the Ring-Opening Polymerization of ε-Caprolactone with 1,8-Diazacyclo[5.4.0]Undec-7-Ene Organocatalyst in Bulk. *Eur. Polym. J.* **2021**, *161*, 110861.
(12) Mezzasalma, L.; Dove, A. P.; Coulembier, O. Organocatalytic Ring-Opening Polymerization of l-Lactide in Bulk: A Long Standing Challenge. *Eur. Polym. J.* **2017**, *95*, 628−634.
(13) Makiguchi, K.; Satoh, T.; Kakuchi, T. Diphenyl Phosphate as an Efficient Cationic Organocatalyst for Controlled/Living Ring-Opening Polymerization of δ-Valerolactone and ε-Caprolactone. *Macromolecules* **2011**, *44*, 1999−2005.
(14) Abbott, A. P.; Capper, G.; Davies, D. L.; Rasheed, R. K.; Tambyrajah, V. Novel solvent properties of choline chloride/urea mixturesElectronic supplementary information (ESI) available: spectroscopic data. See http://www.rsc.org/suppdata/cc/b2/b210714g/. *Chem. Commun.* **2003**, *9*, 70−71.
(15) Mota-Morales, J. D.; Sánchez-Leija, R. J.; Carranza, A.; Pojman, J. A.; del Monte, F.; Luna-Bárcenas, G. Free-Radical Polymerizations of and in Deep Eutectic Solvents: Green Synthesis of Functional Materials. *Prog. Polym. Sci.* **2018**, *78*, 139−153.
(16) Mota-Morales, J. D.; Gutiérrez, M. C.; Sanchez, I. C.; Luna-Bárcenas, G.; Del Monte, F. Frontal Polymerizations Carried out in Deep-Eutectic Mixtures Providing Both the Monomers and the Polymerization Medium. *Chem. Commun.* **2011**, *47*, 5328−5330.
(17) Coulembier, O.; Lemaur, V.; Josse, T.; Minoia, A.; Cornil, J.; Dubois, P. Synthesis of Poly(l-Lactide) and Gradient Copolymers from a l-Lactide/Trimethylene Carbonate Eutectic Melt. *Chem. Sci.* **2012**, *3*, 723−726.
(18) García-Argüelles, S.; García, C.; Serrano, M. C.; Gutiérrez, M. C.; Ferrer, M. L.; Del Monte, F. Near-to-Eutectic Mixtures as Bifunctional Catalysts in the Low-Temperature-Ring-Opening-Polymerization of ε-Caprolactone. *Green Chem.* **2015**, *17*, 3632−3643.
(19) Chen, S.; Wang, H.; Li, Z.; Wei, F.; Zhu, H.; Xu, S.; Xu, J.; Liu, J.; Gebru, H.; Guo, K. Metallic Organophosphate Catalyzed Bulk Ring-Opening Polymerization. *Polym. Chem.* **2018**, *9*, 732−742.
(20) Mosnáček, J.; Duda, A.; Libiszowski, J.; Penczek, S. Copolymerization of LL-Lactide at Its Living Polymer−Monomer Equilibrium with ε-Caprolactone as Comonomer. *Macromolecules* **2005**, *38*, 2027−2029.
(21) Kivijärvi, T.; Pappalardo, D.; Olsen, P.; Finne-Wistrand, A. Inclusion of Isolated α-Amino Acids along the Polylactide Chain through Organocatalytic Ring-Opening Copolymerization. *Eur. Polym. J.* **2020**, *131*, 109703.
(22) Wang, B.; Pan, L.; Ma, Z.; Li, Y. Ring-Opening Polymerization with Lewis Pairs and Subsequent Nucleophilic Substitution: A Promising Strategy to Well-Defined Polyethylene-like Polyesters without Transesterification. *Macromolecules* **2018**, *51*, 836−845.
(23) Wu, D.; Lv, Y.; Guo, R.; Li, J.; Habadati, A.; Lu, B.; Wang, H.; Wei, Z. Kinetics of Sn(Oct)2-Catalyzed Ring Opening Polymerization of ε-Caprolactone. *Macromol. Res.* **2017**, *25*, 1070−1075.
(24) Rudin, A.; Choi, P. *Polymer Science and Engineering*; Academic Press, Elsevier: Boston, MA, USA, 2013, pp 275−304.The Elements Polymer Science and Engineering
(25) Lohmeijer, B. G. G.; Pratt, R. C.; Leibfarth, F.; Logan, J. W.; Long, D. A.; Dove, A. P.; Nederberg, F.; Choi, J.; Wade, C.; Waymouth, R. M.; Hedrick, J. L. Guanidine and Amidine Organocatalysts for Ring-Opening Polymerization of Cyclic Esters. *Macromolecules* **2006**, *39*, 8574−8583.
(26) Wang, X.; Liu, J.; Xu, S.; Xu, J.; Pan, X.; Liu, J.; Cui, S.; Li, Z.; Guo, K. Traceless Switch Organocatalysis Enables Multiblock Ring-Opening Copolymerizations of Lactones, Carbonates, and Lactides: By a One plus One Approach in One Pot. *Polym. Chem.* **2016**, *7*, 6297−6308.
(27) Gagliardi, M.; Bifone, A. Ring-Opening Copolymerization Thermodynamics and Kinetics of γ-Valerolactone/ε-Caprolactone. *PLoS One* **2018**, *13*, 01992311.
(28) Broz, M. E.; VanderHart, D. L.; Washburn, N. R. Structure and Mechanical Properties of Poly(D,L-Lactic Acid)/Poly(ε-Caprolactone) Blends. *Biomaterials* **2003**, *24*, 4181−4190.
(29) Saeed, W.; Al-Odayni, A.-B.; Alghamdi, A.; Alrahlah, A.; Aouak, T. Thermal Properties and Non-Isothermal Crystallization Kinetics of Poly (δ-Valerolactone) and Poly (δ-Valerolactone)/Titanium Dioxide Nanocomposites. *Crystals* **2018**, *8*, 452.
(30) Zhang, D.; Dashtimoghadam, E.; Fahimipour, F.; Hu, X.; Li, Q.; Bersenev, E. A.; Ivanov, D. A.; Vatankhah-Varnoosfaderani, M.; Sheiko, S. S. Tissue-Adaptive Materials with Independently Regulated Modulus and Transition Temperature. *Adv. Mater.* **2020**, *32*, 2005314.
(31) Alghamdi, A. A.; Saeed, W. S.; Al-Odayni, A. B.; Alharthi, F. A.; Semlali, A.; Aouak, T. Poly(Ethylene-Co-Vinylalcohol)/Poly(δ-Valerolactone)/Aspirin Composite: Model for Anewdrug-Carrier System. *Polymers* **2019**, *11*, 439−524.
(32) He, A.; Han, C. C.; Yang, G. Preparation and Characterization of PLLA/P(CL-b-LLA) Blends by an in Situ Ring-Opening Polymerization. *Polymer* **2004**, *45*, 8231−8237.
(33) Han, W.; Liao, X.; Yang, Q.; Li, G.; He, B.; Zhu, W.; Hao, Z. Crystallization and Morphological Transition of Poly(l-Lactide)-Poly(ε-Caprolactone) Diblock Copolymers with Different Block Length Ratios. *RSC Adv.* **2017**, *7*, 22515−22523.
(34) Mofokeng, J. P.; Luyt, A. S. Morphology and Thermal Degradation Studies of Melt-Mixed Poly(Lactic Acid) (PLA)/Poly(ε-Caprolactone) (PCL) Biodegradable Polymer Blend Nanocomposites with TiO2 as Filler. *Polym. Test.* **2015**, *45*, 93−100.
(35) Yin, G.; Zhao, D.; Wang, X.; Ren, Y.; Zhang, L.; Wu, X.; Nie, S.; Li, Q. Bio-Compatible Poly(Ester-Urethane)s Based on PEG-PCL-PLLA Copolymer with Tunable Crystallization and Bio-Degradation Properties. *RSC Adv.* **2015**, *5*, 79070−79080.
(36) Huang, W.; Wen, X.; Zhou, J.; Zhang, X. Understanding the Hydrolysis Mechanism on Segments and Aggregate Structures: Corrosion-Tailored Poly (Lactic Acid) Deriving Copolymers with δ-Valerolactone. *Int. J. Biol. Macromol.* **2022**, *222*, 961−971.
(37) Mishra, G. P.; Kinser, R.; Wierzbicki, I. H.; Alany, R. G.; Alani, A. W. G. In Situ Gelling Polyvalerolactone-Based Thermosensitive Hydrogel for Sustained Drug Delivery. *Eur. J. Pharm. Biopharm.* **2014**, *88*, 397−405.
(38) Fernández, J.; Etxeberria, A.; Sarasua, J. R. In Vitro Degradation of Poly(Lactide/δ-Valerolactone) Copolymers. *Polym. Degrad. Stab.* **2015**, *112*, 104−116.
(39) Saeed, W. S.; Al-Odayni, A. B.; Alrahlah, A.; Alghamdi, A. A.; Aouak, T. Preparation and Characterization of Poly(δ-Valerolactone)/TiO 2 Nanohybrid Material with Pores Interconnected for Potential Use in Tissue Engineering. *Materials* **2019**, *12*, 528.
(40) Athanasoulia, I. G.; Tarantili, P. A. Preparation and Characterization of Polyethylene Glycol/Poly(L-Lactic Acid) Blends. *Pure Appl. Chem.* **2017**, *89*, 141−152.

https://doi.org/10.1021/acsapm.3c00591
ACS Appl. Polym. Mater. 2023, 5, 5110−5121

(41) Tamboli, V.; Mishra, G. P.; Mitra, A. K. Novel Pentablock Copolymer (PLA-PCL-PEG-PCL-PLA) Based Nanoparticles for Controlled Drug Delivery: Effect of Copolymer Compositions on the Crystallinity of Copolymers and in Vitro Drug Release Profile from Nanoparticles. *Colloid Polym. Sci.* **2013**, *291*, 1235−1245.
(42) Doshi, B.; Sillanpää, M.; Kalliola, S. A Review of Bio-Based Materials for Oil Spill Treatment. *Water Res.* **2018**, *135*, 262−277.

https://doi.org/10.1021/acsapm.3c00591
ACS Appl. Polym. Mater. 2023, 5, 5110−5121